SIAM J. SCI. COMPUT.
Vol. 20, No. 3, pp. 878–906

ISSUES RELATED TO LEAST-SQUARES FINITE ELEMENT METHODS FOR THE STOKES EQUATIONS*

JENNIFER M. DEANG† AND MAX D. GUNZBURGER‡

Abstract. Least-squares finite element methods have become increasingly popular for the approximate solution of first-order systems of partial differential equations. Here, after a brief review of some existing theories, a number of issues connected with the use of such methods for the velocity-vorticity-pressure formulation of the Stokes equations in two dimensions in realistic settings are studied through a series of computational experiments. Finite element spaces that are not covered by existing theories are considered; included in these are piecewise linear approximations for the velocity. Mixed boundary conditions, which are also not covered by existing theories, are also considered, as is enhancing mass conservation. Next, problems in nonconvex polygonal regions and the resulting nonsmooth solutions are considered with a view toward seeing how accuracy can be improved. A conclusion that can be drawn from this series of computational experiments is that the use of appropriate mesh-dependent weights in the least-squares functional almost always improves the accuracy of the approximations. Concluding remarks concerning three-dimensional problems, the nonlinear Navier–Stokes equations, and the conditioning of the discrete systems are provided.

Key words. least squares, finite element methods, Stokes equations

AMS subject classification. 65N30

PII. S1064827595294526

1. Introduction.

Least-squares finite element methods have always held out the attraction of yielding discrete linear systems that are symmetric and positive definite even for problems for which other methods, e.g., mixed finite element methods, fail to do so; see, e.g., [2]–[48], [50]–[56], [58], and [60]–[84]. In many settings such as the primitive variable formulation of the Stokes equations, these methods suffer from two serious problems. The first is that conforming discretizations require the use of continuously differentiable finite element functions and the second is that the condition number of the discrete equations is often proportional to h^{-4}, where h denotes some measure of the grid size. However, least-squares finite element methods have recently been receiving increasing attention in both the engineering and mathematics communities; see, e.g., [3], [5]–[15], [17]–[24], [27]–[31], [33]–[44], [46]–[47], [58], [60]–[71], [73], [75]–[80], and [82]–[84]. The focus of this attention has been on the application of least-squares finite element methodologies to first-order systems of partial differential equations for which one can, in principle, use merely continuous finite element functions and for which one may often prove that the condition numbers of the discrete systems are proportional to h^{-2}.

The mathematical references cited above consider least-squares finite element methods in idealized situations, i.e., for problems having simple boundary conditions and smooth solutions and in the asymptotic limit of the grid size measure $h \to 0$. Unfortunately, these are usually far from true in most applications of the methods to practical problems; indeed, there are many such settings for which mathematical

*Received by the editors November 3, 1995; accepted for publication (in revised form) June 10, 1997; published electronically October 20, 1998.

http://www.siam.org/journals/sisc/20-3/29452.html

†Interdisciplinary Center for Applied Mathematics, Virginia Tech, Blacksburg, VA 24061-0531. This research was supported by an NSF Graduate Fellowship.

‡Department of Mathematics, Iowa State University, Ames, IA 50011-2064 (gunzburg@iastate.edu). This research was supported in part by the Air Force Office of Scientific Research grant AFOSR-93-1-0280.

theories have not yet been developed. Often, complex combinations of boundary conditions are needed and solutions are not smooth enough to recover the full accuracy of the finite element functions used. Moreover, often the grid sizes used are not sufficiently small to be in the asymptotic range of mathematical error estimates. In such cases, a naive implementation of least-squares finite element methods may lead, for various reasons, to a deterioration in the expected accuracy of the approximations.

Of course, in some of the engineering literature, practical problems have been considered. However, there the focus has been on obtaining solutions and on efficient implementation of the methods; little attention has again been paid to accuracy and other issues in the presence of complications that are not adequately treated by mathematical theories.

Here, we focus on some of these complications in the context of the stationary Stokes equations in two dimensions. (Most of our observations also apply to other first-order systems of partial differential equations. Certainly, these include the Stokes and Navier–Stokes problems in three dimensions.) In the context of the Navier–Stokes equations, the specific features of least-squares finite element methods that make them potentially advantageous compared with, e.g., mixed and stabilized Galerkin methods, are as follows:

- the choice of approximating spaces is not subject to the Ladyzhenskaya–Babuska–Brezzi (LBB) condition;
- a single approximating space can be used for all variables;
- solution methods can be devised that require no matrix assemblies, even at the element level;
- used in conjunction with Newton linearization results in symmetric, positive definite linear systems, at least in the neighborhood of a solution;
- used in conjunction with properly implemented continuation (with respect to the Reynolds number) techniques, a solution method can be devised that will only encounter symmetric, positive definite linear systems;
- standard and robust iterative methods for symmetric, positive definite linear systems can be used;
- essential boundary conditions can be handled easily;
- no artificial boundary conditions for the vorticity need be introduced at boundaries at which the velocity is specified; and
- accurate vorticity approximations are obtained.

(For a discussion of the LBB condition, see, e.g., [57] or [59].) This list of advantages is formidable and certainly justifies the recent increased interest garnered by least-squares finite element methods for fluids applications. However, as mentioned above, there are still some unresolved issues that must be addressed and solved before such methods become truly practical. Through some computational experiments we show how the methods behave in various settings that arise in practical computations. Whenever we find that the performance of the methods deviates from that which is attainable in the idealized settings treated by the mathematical theories, we offer some remedies that at least partially lessen the deterioration.

For the sake of completeness, we begin, in section 2, with a review of existing theories for least-squares finite element methods for the Stokes equations in two dimensions. Then, in section 3, we present the results of our studies into some of the issues that arise when these methods are implemented in practical settings. In section 4, we give some concluding remarks that include some brief comments on three-dimensional calculations and on the Navier–Stokes equations.

2. Review of the theory. The generalized stationary Stokes problem in an open, bounded two-dimensional domain Ω with boundary Γ is given by

$$-\Delta \mathbf{u} + \mathbf{grad}\, \widehat{p} = \mathbf{f}_1 \qquad \text{in } \Omega\,, \tag{2.1}$$

$$\operatorname{div} \mathbf{u} = f_2 \qquad \text{in } \Omega\,, \tag{2.2}$$

and

$$\mathbf{u} = \mathbf{U} \qquad \text{on } \Gamma\,, \tag{2.3}$$

where $\mathbf{u}$ and $\widehat{p}$ denote the velocity and pressure fields, respectively, and where $\mathbf{f}_1$, f_2, and $\mathbf{U}$ denote given functions. This system is referred to as the *primitive variable formulation.* Although least-squares methodologies may be defined for (2.1)–(2.3), e.g., see [2], they do not lead to practical methods.

The great majority of work on least-squares finite element methods for the Stokes problem is based on the *velocity-vorticity-"pressure"* formulation, which for the generalized Stokes problem is given by the first-order system of differential equations

$$\mathbf{curl}\, \omega + \mathbf{grad}\, p = \mathbf{f}_1 \qquad \text{in } \Omega\,, \tag{2.4}$$

$$\operatorname{div} \mathbf{u} = f_2 \qquad \text{in } \Omega\,, \tag{2.5}$$

and

$$\operatorname{curl} \mathbf{u} - \omega = f_3 \qquad \text{in } \Omega, \tag{2.6}$$

along with (2.3), where ω and $p = \widehat{p} + |\mathbf{u}|^2/2$ denote the vorticity field and the total pressure, respectively, and where f_3 denotes another given function. For steady Stokes flow, one has that $f_2 = f_3 = 0$. With $f_3 = 0$, one easily finds that the system (2.3)–(2.6) is equivalent to the system (2.1)–(2.3).

For the sake of simplicity, we consider the homogeneous versions of (2.3), i.e.,

$$\mathbf{u} = \mathbf{0} \qquad \text{on } \Gamma\,. \tag{BC1}$$

We also compare and contrast (BC1) with another set of boundary conditions, namely,

$$\mathbf{u} \cdot \mathbf{n} = 0 \qquad \text{and} \qquad p = 0 \qquad \text{on } \Gamma\,. \tag{BC2}$$

We assume that the data satisfy all necessary compatibility conditions, e.g.,

$$\int_\Omega f_2 \, d\Omega = 0\,.$$

The analyses of least-squares finite element methods is carried out in a *Sobolev space* setting. To this end, we introduce the spaces

$$H^m(\Omega) = \left\{ \begin{array}{l} \text{set of functions such that all} \\ \text{partial derivatives of order} \\ \leq m \text{ are square integrable} \end{array} \right\}\,.$$

A norm for a function g belonging to $H^m(\Omega)$ is provided by

$$\|g\|_m^2 = \sum_{m_1+m_2 \leq m} \int_\Omega \left(\frac{\partial^{(m_1+m_2)} g}{\partial x^{m_1} \partial y^{m_2}} \right)^2 \, d\Omega\,.$$

2.1. Elements of the Agmon–Douglis–Nirenberg (ADN) theory. The analyses of least-squares finite element methods is based on the *ADN theory* for elliptic partial differential equations [1]. Some key features of this theory are summarized as follows.

- The ADN theory yields a priori estimates for solutions of elliptic boundary value problems.
- The norms appearing in the estimates are chosen so that the differential operator and boundary condition operator satisfy a certain precise condition known as the *complementing condition.*
- If the differential operator is elliptic, and the complementing condition is satisfied, we call the system of partial differential equations and boundary conditions an *ADN system.*
- For the same system of differential equations, different boundary conditions may result in the usage of different norms within the ADN theory; i.e., a system of partial differential equations and boundary conditions may be an ADN system with respect to different norms than the same partial differential equations with different boundary conditions.
- The correct ADN norms are related to the principal part of the differential operator; e.g., the principal part of the operator determines the well-posedness of the problem.

For the *pressure-normal velocity* boundary condition (BC2), the principal part of the Stokes operator is given by

$$\begin{aligned} \mathbf{curl}\,\omega + \mathbf{grad}\,p, \\ \operatorname{curl}\mathbf{u}, \\ \operatorname{div}\mathbf{u}\,. \end{aligned}$$

Note that only first derivatives terms appear in the principal part. As a result, one has that all variables have the same differentiability properties. The principal part operator along with the boundary conditions uncouple into the two well-posed problems

$$\begin{aligned} \mathbf{curl}\,\omega + \mathbf{grad}\,p = \mathbf{f}_1 \quad &\text{in } \Omega, \\ p = P \quad &\text{on } \Gamma, \end{aligned}$$

and

$$\begin{aligned} \operatorname{div}\mathbf{u} = f_2 \quad \text{and} \quad \operatorname{curl}\mathbf{u} = f_3 \quad &\text{in } \Omega, \\ \mathbf{u}\cdot\mathbf{n} = U_n \quad &\text{on } \Gamma\,. \end{aligned}$$

The ADN a priori estimate relevant to least-squares methods is given by

$$\|\omega\|_1 + \|p\|_1 + \|\mathbf{u}\|_1 \le C\left(\|\mathbf{f}_1\|_0 + \|f_2\|_0 + \|f_3\|_0\right)\,.$$

Note that all norms on the components of the solution are the same and that also all the components of the data are measured in a single norm.

If, for the *velocity* boundary condition (BC1), one arbitrarily chooses the same principal part as before, we see that the principal part operator along with the boundary condition uncouple into the two problems

$$\mathbf{curl}\,\omega + \mathbf{grad}\,p = \mathbf{f}_1 \quad \text{in } \Omega$$

and

$$\begin{aligned} \operatorname{div}\mathbf{u} = f_2 \quad \text{and} \quad \operatorname{curl}\mathbf{u} = f_3 \quad &\text{in } \Omega, \\ \mathbf{u} = \mathbf{U} \quad &\text{on } \Gamma\,. \end{aligned}$$

These problems are not well posed; i.e., the first is underdetermined (not enough boundary conditions), and the second is overdetermined (too many boundary conditions).

The ADN theory tells us that the correct principal part of the Stokes operator with velocity boundary conditions is given by

$$\begin{aligned} \mathbf{curl}\,\omega + \mathbf{grad}\,p, \\ \operatorname{div}\mathbf{u}, \\ -\omega + \operatorname{curl}\mathbf{u}, \end{aligned}$$

so that the principal part is the whole operator. The third operator in this principal part implies that $\mathbf{u}$ and ω cannot have the same differentiability properties. For the case of (BC1), the ADN a priori estimate relevant to least-squares methods is now given by

$$\|\omega\|_1 + \|p\|_1 + \|\mathbf{u}\|_2 \le C\left(\|\mathbf{f}_1\|_0 + \|f_2\|_1 + \|f_3\|_1\right)\,.$$

Note that different components of the solution are measured in different norms and that the different components of the data are also measured in different norms. Note also the consistency achieved by the ADN theory. If $\mathbf{u}$ has two square integrable derivatives, then ω and p have one square integrable derivative. Then the combination $\mathbf{curl}\,\omega + \mathbf{grad}\,p$, i.e., $\mathbf{f}_1$, should be merely square integrable, and the combinations $\operatorname{div}\mathbf{u}$ and $\operatorname{curl}\mathbf{u} - \omega$, i.e., f_2 and f_3, respectively, should have one square integrable derivative. These are exactly the norms appearing in the a priori estimate.

If one uses the same norm for all unknowns (and also the same norm for all the data), then, in the velocity boundary condition case, the Stokes system is *not* an ADN system, i.e., the system is not well posed with respect to those norms.

2.2. Least-squares methods for the normal velocity-pressure BC case (BC2). A least-squares functional can be set up by summing up the squares of the residuals of the equations

$$\mathcal{J}(\mathbf{u}, p, \omega) = \|\mathbf{curl}\,\omega + \mathbf{grad}\,p - \mathbf{f}_1\|^2 + \|\operatorname{div}\mathbf{u} - f_2\|^2 + \|\operatorname{curl}\mathbf{u} - \omega - f_3\|^2\,.$$

The natural question is, What norms should be used to measure the size of the residuals? An answer is given as follows. If one uses the norms indicated by the ADN theory and if one also uses a conforming finite element method, then, from a *practical point of view*, optimally accurate solutions are obtained for all variables; furthermore, from a *mathematical point of view*, the analysis of errors, e.g., the derivation of rigorous error estimates, is completely straightforward.

Thus, the least-squares functional for the normal velocity-pressure BC case is given by

$$\begin{aligned} \mathcal{J}(\mathbf{u}, p, \omega) &= \|\mathbf{curl}\,\omega + \mathbf{grad}\,p - \mathbf{f}_1\|_0^2 + \|\operatorname{div}\mathbf{u} - f_2\|_0^2 + \|\operatorname{curl}\mathbf{u} - \omega - f_3\|_0^2 \\ &= \int_\Omega |\mathbf{curl}\,\omega + \mathbf{grad}\,p - \mathbf{f}_1|^2 \, d\Omega + \int_\Omega (\operatorname{div}\mathbf{u} - f_2)^2 \, d\Omega \\ &\qquad + \int_\Omega (\operatorname{curl}\mathbf{u} - \omega - f_3)^2 \, d\Omega\,. \end{aligned}$$

Note that this functional involves at most products of *first* derivatives. The least-squares principle is then given by the following:

seek $(\mathbf{u}, p, \omega)$ *such that* $\mathcal{J}$ *is minimized over an appropriate class of functions* $\mathcal{V}$.

The function class $\mathcal{V}$ consists of $H^1(\Omega)$ velocity, pressure, and vorticity fields, constrained by boundary conditions, etc. The Euler–Lagrange equations corresponding to the least-squares principle are given by

$$\textit{seek } (\mathbf{u}, p, \omega) \in \mathcal{V} \textit{ such that } \mathcal{B}\big((\mathbf{u}, p, \omega)\,,\,(\mathbf{v}, q, \xi)\big) = \mathcal{F}(\mathbf{v}, q, \xi) \quad \textit{for all } (\mathbf{v}, q, \xi) \in \mathcal{V}\,,$$

where

$$\mathcal{B}\big((\mathbf{u}, p, \omega)\,,\,(\mathbf{v}, q, \xi)\big) = \int_\Omega (\mathbf{curl}\,\omega + \mathbf{grad}\,p)\cdot(\mathbf{curl}\,\xi + \mathbf{grad}\,q)\,d\Omega + \int_\Omega (\operatorname{div}\mathbf{u})(\operatorname{div}\mathbf{v})\,d\Omega + \int_\Omega (\operatorname{curl}\mathbf{u} - \omega)(\operatorname{curl}\mathbf{v} - \xi)\,d\Omega$$

and

$$\mathcal{F}(\mathbf{v}, q, \xi) = \int_\Omega \mathbf{f}_1\cdot(\mathbf{curl}\,\xi + \mathbf{grad}\,q)\,d\Omega + \int_\Omega f_2 \operatorname{div}\mathbf{v}\,d\Omega + \int_\Omega f_3(\operatorname{curl}\mathbf{v} - \xi)\,d\Omega\,.$$

Finite element approximations are now defined in a standard manner. First, choose a conforming finite element approximating space $\mathcal{V}^h$; i.e., choose the finite element functions for all variables so that their derivatives are square integrable. Then seek $(\mathbf{u}^h, p^h, \omega^h) \in \mathcal{V}^h$ such that

$$\mathcal{B}\big((\mathbf{u}^h, p^h, \omega^h)\,,\,(\mathbf{v}^h, q^h, \xi^h)\big) = \mathcal{F}(\mathbf{v}^h, q^h, \xi^h) \quad \text{for all } (\mathbf{v}^h, q^h, \xi^h) \in \mathcal{V}^h\,.$$

This problem is equivalent to a linear algebraic system having a symmetric, positive definite coefficient matrix. Standard finite element methodology, i.e., based on the Lax–Milgram theorem, can be used to derive *optimal error estimates.* For example, if piecewise linear polynomials are used for all variables (and the exact solution is sufficiently smooth), one finds that

$$\|\mathbf{u} - \mathbf{u}^h\|_1 + \|p - p^h\|_1 + \|\omega - \omega^h\|_1 = O(h)\,; \tag{2.7}$$

if piecewise quadratic polynomials are used, one instead finds that

$$\|\mathbf{u} - \mathbf{u}^h\|_1 + \|p - p^h\|_1 + \|\omega - \omega^h\|_1 = O(h^2)\,. \tag{2.8}$$

Note that

- all variables are approximated by the same finite element functions;
- all variables are optimally approximated; and
- conforming finite element approximations for all variables are required to be merely continuous across element edges.

2.3. Least-squares finite element methods for the velocity BC case (BC1) using ADN norms. The least-squares functional for the velocity boundary condition case (BC1) using the norms indicated by the ADN theory is given by

$$\begin{aligned}\mathcal{K}(\mathbf{u}, p, \omega) &= \|\mathbf{curl}\,\omega + \mathbf{grad}\,p - \mathbf{f}_1\|_0^2 + \|\operatorname{div}\mathbf{u} - f_2\|_1^2 + \|\operatorname{curl}\mathbf{u} - \omega - f_3\|_1^2 \\ &= \int_\Omega |\mathbf{curl}\,\omega + \mathbf{grad}\,p - \mathbf{f}_1|^2\,d\Omega \\ &\qquad + \int_\Omega \Big(|\operatorname{grad}\,(\operatorname{div}\mathbf{u} - f_2)|^2 + (\operatorname{div}\mathbf{u} - f_2)^2\Big)\,d\Omega \\ &\qquad + \int_\Omega \Big(|\operatorname{grad}\,(\operatorname{curl}\mathbf{u} - \omega - f_3)|^2 + (\operatorname{curl}\mathbf{u} - \omega - f_3)^2\Big)\,d\Omega\,.\end{aligned}$$

Note that this functional involves products of *second* derivatives of the velocity. The least-squares principle is then given by the following:

seek $(\mathbf{u}, p, \omega)$ *such that* $\mathcal{K}$ *is minimized over an appropriate class of functions* $\mathcal{W}$.

The function class $\mathcal{W}$ now consists of $H^1(\Omega)$ pressure and vorticity fields and $H^2(\Omega)$ velocity fields, constrained by boundary conditions, etc. The Euler–Lagrange equation for this least-squares principle again has the form

$$\text{seek } (\mathbf{u}, p, \omega) \in \mathcal{W} \text{ such that } \widetilde{\mathcal{B}}\big((\mathbf{u}, p, \omega)\,, (\mathbf{v}, q, \xi)\big) = \widetilde{\mathcal{F}}(\mathbf{v}, q, \xi) \quad \text{for all } (\mathbf{v}, q, \xi) \in \mathcal{W}\,,$$

where $\widetilde{\mathcal{B}}(\cdot, \cdot)$ is a bilinear form that involves products of second derivatives of $\mathbf{u}$ and $\mathbf{v}$.

Finite element approximations can then be defined in a standard manner as follows. First, choose a conforming finite element approximating space $\mathcal{W}^h$; i.e., choose the finite element functions for approximating the pressure and vorticity so that their derivatives are square integrable and choose finite element functions for approximating the velocity so that their *second* derivatives are square integrable. Then seek $(\mathbf{u}^h, p^h, \omega^h) \in \mathcal{W}^h$ such that

$$\widetilde{\mathcal{B}}\big((\mathbf{u}^h, p^h, \omega^h)\,, (\mathbf{v}^h, q^h, \xi^h)\big) = \widetilde{\mathcal{F}}(\mathbf{v}^h, q^h, \xi^h) \quad \text{for all } (\mathbf{v}^h, q^h, \xi^h) \in \mathcal{W}^h\,.$$

This problem is again equivalent to a linear algebraic system having a symmetric, positive definite coefficient matrix. Standard finite element methodology, i.e., based on the Lax–Milgram theorem, can be used to derive optimal error estimates whenever conforming finite element spaces are used.

Unfortunately, this method for the velocity boundary condition (BC1) *is not practical*. The requirement that finite element velocity approximations possess two square integrable derivatives forces one to use finite element functions that are *continuously differentiable* across element edges. By the way, if one is willing to use continuously differentiable velocity approximations, one might as well have applied least-squares principles to the primitive variable formulation (2.1)–(2.3)!

2.4. A practical least-squares finite element method for the velocity BC case (BC1). At this point we are faced with the following scenario.

- The dilemma:
  - If, for the velocity boundary condition case (BC1), we use a least-squares functional based on the ADN norms, we are led to a computational method requiring continuously differentiable velocity approximations; i.e., $\Longrightarrow$ *we get an impractical method.*
  - If, on the other hand, we use the more practical functional $\mathcal{J}$ that works easily and optimally for the normal velocity-pressure boundary conditions, $\Longrightarrow$*we get nonoptimal approximations.*
- The question
  - Is there a way to use the simpler and more practical norms of the functional $\mathcal{J}$ and still get optimally accurate approximations?
- The answer:
  - It can be done if one uses *mesh-dependent weights* in the least-squares functional.

The residual norms of the equations that, for practical reasons, we would like to use are given by

$$\|\mathbf{curl}\,\omega + \mathbf{grad}\,p - \mathbf{f}_1\|_0\,, \qquad \|\mathrm{div}\,\mathbf{u} - f_2\|_0\,, \qquad \text{and} \qquad \|\mathrm{curl}\,\mathbf{u} - \omega - f_3\|_0\,; \tag{2.9}$$

the residual norms that, for mathematical reasons, the ADN theory would like us to use are given by

$$\|\mathbf{curl}\,\omega + \mathbf{grad}\,p - \mathbf{f}_1\|_0\,, \qquad \|\mathrm{div}\,\mathbf{u} - f_2\|_1\,, \qquad \text{and} \qquad \|\mathrm{curl}\,\mathbf{u} - \omega - f_3\|_1\,. \tag{2.10}$$

We will introduce weights so that the second and third residuals using the practical norms of (2.9) can be used instead of the corresponding impractical norms of (2.10).

In order to motivate the choice of weights in the practical least-squares functional, we need to recall the notion of *inverse inequalities* for finite element spaces; see, e.g., [49]. The inverse inequality relevant to our discussion is

$$\|q^h\|_1 \le Ch^{-1}\|q^h\|_0\,,$$

where h is an appropriate measure of the grid size and q^h is a function belonging to a regular finite element subspace of $H^1(\Omega)$. This inequality suggests that, for finite element functions, one can "simulate" the norm $\|q^h\|_1$ by $h^{-1}\|q^h\|_0$.

Thus, we are led to the weighted least-squares functional for the velocity boundary condition case (BC1):

$$\begin{aligned}\mathcal{J}_h(\mathbf{u},p,\omega) &= \|\mathbf{curl}\,\omega + \mathbf{grad}\,p - \mathbf{f}_1\|_0^2 + h^{-2}\|\mathrm{div}\,\mathbf{u} - f_2\|_0^2 + h^{-2}\|\mathrm{curl}\,\mathbf{u} - \omega - f_3\|_0^2 \\ &= \int_\Omega |\mathbf{curl}\,\omega + \mathbf{grad}\,p - \mathbf{f}_1|^2\,d\Omega + \frac{1}{h^2}\int_\Omega (\mathrm{div}\,\mathbf{u} - f_2)^2\,d\Omega \\ &\qquad + \frac{1}{h^2}\int_\Omega (\mathrm{curl}\,\mathbf{u} - \omega - f_3)^2\,d\Omega\,.\end{aligned}$$

The least-squares principle is now given by the following:

seek $(\mathbf{u},p,\omega)$ *such that* $\mathcal{J}_h$ *is minimized over an appropriate class of functions* $\mathcal{V}$.

The function class $\mathcal{V}$ again consists of $H^1(\Omega)$ velocity, pressure, and vorticity fields, constrained by boundary conditions, etc. The Euler–Lagrange equations corresponding to this least-squares principle are given by

seek $(\mathbf{u},p,\omega)\in\mathcal{V}$ *such that* $\mathcal{B}_h\big((\mathbf{u},p,\omega)\,,(\mathbf{v},q,\xi)\big) = \mathcal{F}_h(\mathbf{v},q,\xi)$ *for all* $(\mathbf{v},q,\xi)\in\mathcal{V}$,

where

$$\begin{aligned}\mathcal{B}_h\big((\mathbf{u},p,\omega)\,,(\mathbf{v},q,\xi)\big) &= \int_\Omega (\mathbf{curl}\,\omega + \mathbf{grad}\,p)\cdot(\mathbf{curl}\,\xi + \mathbf{grad}\,q)\,d\Omega \\ &\qquad + \frac{1}{h^2}\int_\Omega (\mathrm{div}\,\mathbf{u})(\mathrm{div}\,\mathbf{v})\,d\Omega + \frac{1}{h^2}\int_\Omega (\mathrm{curl}\,\mathbf{u} - \omega)(\mathrm{curl}\,\mathbf{v} - \xi)\,d\Omega\end{aligned}$$

and

$$\mathcal{F}_h(\mathbf{v},q,\xi) = \int_\Omega \mathbf{f}_1\cdot(\mathbf{curl}\,\xi + \mathbf{grad}\,q)\,d\Omega + \frac{1}{h^2}\int_\Omega f_2\mathrm{div}\,\mathbf{v}\,d\Omega + \frac{1}{h^2}\int_\Omega f_3(\mathrm{curl}\,\mathbf{v} - \xi)\,d\Omega\,.$$

Finite element approximations are now defined in a standard manner. First, choose a conforming finite element approximating space $\mathcal{V}^h$; i.e., choose the finite element functions for all variables so that their derivatives are square integrable. Then seek $(\mathbf{u}^h,p^h,\omega^h)\in\mathcal{V}^h$ such that

$$\mathcal{B}_h\big((\mathbf{u}^h,p^h,\omega^h)\,,(\mathbf{v}^h,q^h,\xi^h)\big) = \mathcal{F}_h(\mathbf{v}^h,q^h,\xi^h) \quad \text{for all } (\mathbf{v}^h,q^h,\xi^h)\in\mathcal{V}^h\,.$$

This problems is equivalent to a linear algebraic system having a symmetric, positive definite coefficient matrix.

This method was analyzed in [11]. These analyses suggest that one may use polynomials of one degree lower for the pressure and vorticity than one uses for the velocity. If we use continuous piecewise quadratic polynomials for the velocity approximations and piecewise linear polynomials for the pressure and vorticity approximations, we get the estimate

$$\|\mathbf{u} - \mathbf{u}^h\|_1 + \|p - p^h\|_0 + \|\omega - \omega^h\|_0 = O(h^2)\,. \tag{2.11}$$

This estimate is optimal with respect to the finite element functions used. The theory also says that one may use the same degree polynomials for all variables. For example, if one uses continuous piecewise quadratic polynomials for all variables, one again obtains the above error estimate. In this case, the above estimate is not optimal for the pressure and vorticity.

Thus, we are again led to a simple, easy-to-implement algorithm; i.e.,

- one can use merely continuous finite element functions for all variables;
- one still obtains a symmetric, positive definite discrete linear system; and
- one obtains optimally accurate approximations. However, optimal accuracy is achieved with respect to norms dictated by the ADN theory for the velocity boundary condition case.

2.5. Other first-order formulations for the Stokes equations. The velocity-vorticity-pressure formulation is not the only possible first-order formulation for the Stokes problem (2.1)–(2.3). Another possibility is the *velocity-pressure-stress formulation*. Although this formulation involves more unknowns than does the velocity-vorticity-pressure formulation, it has the advantage that the components of the stress tensor are computed directly. In the velocity-vorticity-pressure formulation, the stress tensor is recovered by differentiating the components of the velocity vector. Least-squares finite element methods based on the velocity-pressure-stress formulation are considered in [13]. A third first-order formulation for the Stokes equations is discussed in [33].

In [8] and [20], a least-squares finite element method for the Stokes and Navier–Stokes equations with velocity boundary conditions was introduced that, without the need of introducing mesh-dependent weights, results in a least-squares functional employing only $L^2(\Omega)$-norms. This method is based on the *velocity-pressure-gradient of velocity formulation* given by the differential equations

$$\underline{U} - (\nabla \mathbf{u})^T = \underline{0} \qquad \text{in } \Omega\,,$$

$$-(\nabla \cdot \underline{U})^T + \mathbf{grad}\, p = \mathbf{f} \qquad \text{in } \Omega\,,$$

$$\operatorname{div} \mathbf{u} = 0 \qquad \text{in } \Omega\,,$$

$$\mathbf{grad}\,(\operatorname{trace} \underline{U}) = \mathbf{0} \qquad \text{in } \Omega\,,$$

and

$$\nabla \times \underline{U} = \underline{0} \qquad \text{in } \Omega$$

and boundary conditions

$$\mathbf{u} = \mathbf{0} \qquad \text{on } \Gamma$$

and

$$\mathbf{n} \times \underline{U} = \underline{0} \qquad \text{on } \Gamma\,.$$

The unknown fields is the nonsymmetric tensor $\underline{U}$, the vector $\mathbf{u}$, and the scalar p. Although this method is of considerable theoretical importance, its practical impact may be limited. An obvious disadvantage of the method is that, in three dimensions, it requires 13 unknowns fields as opposed to 7 fields for the velocity-vorticity-pressure formulation. On the other hand, in principle, one does not have to introduce any mesh-dependent weights in order to get a viable discretization method. However, this observation is valid only for simple problems or for mesh sizes that are too small to be used in practice. In section 3, we will often find that when complications are introduced into a problem that mesh-dependent weights can serve to also ameliorate the impact of those complications. Thus, it seems likely that mesh-dependent weights will be part of practical implementations of any least-squares finite element method for the Stokes or Navier–Stokes equations. For this reason, and also because least-squares finite element methods based on the velocity-vorticity-pressure formulation are by far the most used in engineering practice, we will concentrate on practical issues connected with the implementation of that method.

3. Computational study of practical implementation issues. We now consider a series of issues that arise when least-squares finite element methods are used in practical settings. These issues relate to settings which are, for the most part, not covered by existing theories. Since the issues we discuss are not related to the nonlinearity of the Navier–Stokes equations and are not peculiar to three-dimensional geometries, we will use the generalized velocity-vorticity-pressure formulation of the two-dimensional Stokes equations given by (2.4)–(2.6) as the basis for our computational studies.

Unless otherwise noted, the results we report on are for the exact solution

$$u = v = \sin(\pi x)\sin(\pi y)\,, \tag{3.1}$$

$$\omega = \sin(\pi x)\exp(\pi y)\,, \tag{3.2}$$

and

$$p = \cos(\pi x)\exp(\pi y)\,. \tag{3.3}$$

The data functions $\mathbf{f}_1$, f_2, and f_3 are determined by substituting (3.1)–(3.3) into (2.4)–(2.6).

Possibly inhomogeneous versions of the two types of boundary conditions (BC1) and (BC2) are considered; furthermore, we will also examine cases for which these boundary conditions are applied on disjoint parts of the boundary Ω. Thus, if Γ_{BC1} and Γ_{BC2} denote two disjoint parts of the boundary Γ such that $\Gamma_{BC1} \cup \Gamma_{BC2} = \Gamma$, we specify the boundary conditions

$$\mathbf{u} = \mathbf{U} \quad \text{on } \Gamma_{BC1} \tag{BC1}$$

and

$$\mathbf{u} \cdot \mathbf{n} = U_n \quad \text{and} \quad p = P \quad \text{on } \Gamma_{BC2} \tag{BC2}$$

TABLE 1
Convergence rates for quadratic-quadratic approximations.

	L^2 error rates				H^1 error rates			
Function	BC1	BC1w	BC2	BC2w	BC1	BC1w	BC2	BC2w
u	2.61	3.76	3.14	3.10	1.90	2.19	2.04	2.04
v	2.34	3.32	3.13	3.09	2.02	2.13	2.02	2.02
w	2.10	3.52	3.00	2.94	1.57	2.39	1.91	1.90
p	2.41	3.22	2.97	2.97	1.57	2.40	1.96	1.96

for a given vector-valued function $\mathbf{U}$ defined on Γ_{BC1} and given functions U_n and P defined on Γ_{BC2}. If $\Gamma = \Gamma_{BC1}$, then, for the solution to be unique, an additional constraint must be imposed on the pressure such as requiring the pressure to have zero mean over Ω. The boundary condition (BC2) is not necessarily useful in the context of viscous flows; we consider it here merely to compare and contrast the behavior of least-squares finite element methods for each of the two boundary conditions (BC1) and (BC2). Whenever inhomogeneous boundary conditions are applied, interpolants of the given data in the corresponding finite element spaces are used. The use of interpolants does not seem to affect the convergence behavior of the approximations.

Unless otherwise noted, all our computations are for a unit square domain, i.e., $\Omega = (0,1) \times (0,1)$. Note that in this case we have, for the exact solution (3.1)–(3.3), that $\mathbf{U} = \mathbf{0}$ and $U_n = 0$. In all cases, Ω is subdivided into triangular finite elements. Unless otherwise noted, uniform grids are used. The calculations for the unit square domain are done on a sequence of $n \times n$ grids with $n = 2, 3, \ldots, 20$. Using the results from all these grids, a linear regression is used to calculate rates of convergence. Some of the reported rates of convergence are well above the optimal rates; this is probably due to the fact that the linear regressions used to calculate the rates include calculated results obtained on coarse grids. However, for the calculations reported on here, we have found this method for computing rates to be more reliable than using only the two finest grids, i.e., $n = 19$ and 20, or using the two finest nested grids, i.e., $n = 10$ and 20.

We will study least-squares finite element methods based on both the weighted and unweighted functionals $\mathcal{J}$ and $\mathcal{J}_h$, respectively. Whenever the weighted functional is used, we will append a "w" to the boundary conditions designator; e.g., if we use the weighted functional with boundary condition BC1, we will denote that case by BC1w.

3.1. Quadratic-quadratic finite element spaces. In this section, we use continuous piecewise quadratic polynomials for all four variables, i.e., for the two components of the velocity, the vorticity, and the pressure. The use of a single approximating space for all variables simplifies programming of least-squares finite element methods. The computational results are obtained for the exact solution (3.1)–(3.3) on a unit square domain. In Table 1 are listed rates of convergence (with respect to the grid size) determined from errors computed on different grids for various combinations of boundary conditions and functionals.

We first study the case for which the boundary condition (BC2) is applied on all of Γ and for which we use the functional $\mathcal{J}$ as the basis for the least-squares finite element method. In this case, with the use of quadratic finite element functions for all four variables, one expects from (2.8) that the approximations to all four variables converge at a second-order rate in the H^1-norm. This is confirmed by the results listed in the BC2 columns of Table 1. Note also the third-order rate for the error

measured in the L^2-norm.

Next, we stay with the boundary condition (BC2) applied on all of Γ, but now we use the weighted functional $\mathcal{J}_h$ as the basis for the least-squares finite element method. This case is not covered by the theories of section 2. However, we see from the BC2w columns of Table 1 that the accuracy of the approximations for this case is nearly the same as for the previous case wherein we used (BC2) on all of Γ along with the functional $\mathcal{J}$. Thus, the use of mesh-dependent weights does not seem to affect the accuracy of quadratic-quadratic approximations for the case (BC2).

Now we turn to cases for which the boundary condition (BC1) is applied on all of the boundary. The theories of section 2 do not apply to this boundary condition if one uses the unweighted functional $\mathcal{J}$. From the BC1 columns of Table 1, one sees that the rates of convergence for this combination are not all optimal. The H^1-norm rates are probably more reliable indicators of what happens in general. There we see that there is a slight loss of accuracy for the vorticity and pressure approximations; i.e., one does not recover the full second-order accuracy of the quadratic finite element functions used.

If instead we use the weighted functional $\mathcal{J}_h$ along with the boundary condition (BC1) on all of Γ, the theory of section 2.4 results in the error estimate (2.11). Thus, the error estimate predicts that one obtains optimal second-order convergence for velocity approximations in the H^1-norm. For vorticity and pressure approximations, this estimate only predicts that the L^2-norm convergence rates are no worse than second-order, which is suboptimal for the quadratic finite element functions used. However, from the BC1w columns of Table 1, we see that one does better than that for the vorticity and pressure.

The conclusion that can be reached is that the use of quadratic finite element functions for all variables yields optimal accurate approximations whenever (BC1) or (BC2) is applied on all of the boundary, so long as the weighted functional is used for the case (BC1).

3.2. Quadratic-linear finite element spaces. In Table 2, we give computed convergence rates using continuous piecewise quadratic finite element functions for the velocity component approximations and continuous piecewise linear finite element functions for the vorticity and pressure approximations. The error estimates (2.11) for the case BC1w were valid for quadratic or linear approximations of the vorticity and pressure. As previously noted in Table 1, using quadratic approximations for p and ω yields a higher rate of convergence for BC1w than predicted by (2.11). The use of linear approximations for the vorticity and pressure should mimic more closely the theoretical result (2.11) for the BC1w case. In fact, examination of the BC1w columns in Table 2 indicates that indeed the H^1 errors of the velocity components and the L^2 errors of the vorticity and pressure are all of $O(h^2)$, as predicted by (2.11). The H^1 rate of convergence for the vorticity and pressure approximations seems to be optimal for the linear functions used for these variables.

Looking at the BC1 columns of Table 2, we see that using quadratic approximations for the velocity and linear approximations for the vorticity and pressure results in a disastrous loss of accuracy with respect to both the H^1 and L^2 errors. The BC2 and BC2w columns are nearly identical; they indicate that the accuracy is severely compromised, especially for the quadratic velocity approximations.

The conclusion that can be drawn from Table 2 is that quadratic-linear approximations can only be used in the BC1w case for which the theory leading to the error estimate (2.11) applies. Otherwise, one gets substantially less accuracy than possible

TABLE 2
Convergence rates for quadratic-linear approximations.

	L^2 error rates				H^1 error rates			
Function	BC1	BC1w	BC2	BC2w	BC1	BC1w	BC2	BC2w
u	0.12	2.00	0.92	0.92	0.14	1.91	1.03	1.02
v	0.15	2.54	0.92	0.91	0.14	2.18	1.08	1.08
w	0.17	2.01	1.14	1.13	0.16	1.22	0.91	0.91
p	0.29	1.98	1.96	1.96	0.16	1.21	0.91	0.96

TABLE 3
Convergence rates for linear-linear approximations.

	L^2 error rates				H^1 error rates			
Function	BC1	BC1w	BC2	BC2w	BC1	BC1w	BC2	BC2w
u	0.24	1.83	1.25	0.82	0.17	1.12	0.93	0.78
v	0.29	2.08	1.29	0.87	0.12	1.13	0.93	0.79
w	0.19	2.01	1.49	0.83	0.17	1.20	0.91	0.88
p	0.22	1.66	1.96	1.96	0.17	1.19	0.96	0.96

with the finite element functions used.

3.3. Linear-linear finite element spaces. The theory for the pressure-normal velocity boundary condition (BC2) and the unweighted functional $\mathcal{J}$ that led to the error estimate (2.7) applies to continuous piecewise linear velocity approximations along with like approximations for the vorticity and pressure. However, the theory for the velocity boundary condition and the weighted functional $\mathcal{J}_h$ that led to the error estimate (2.11) does not apply to this choice of approximating functions for the velocity. Thus, our next computational study is to determine convergence rates for this linear-linear case and for the various combinations of boundary conditions and functionals. The results are given in Table 3.

Very poor rates result when the boundary condition (BC1) is combined with the unweighted functional $\mathcal{J}$. Use of the weighted functional $\mathcal{J}_h$ seems to yield good convergence rates; indeed, with respect to the H^1-norm these seem to be optimal. The rates for the boundary condition (BC2) combined with the unweighted functional $\mathcal{J}$ confirm the theoretical results of (2.7). In this case, it seems that the use of weights hurts the accuracy of the approximations for the normal velocity-pressure boundary condition case.

The conclusion that can be drawn from these results is that linear approximations for the velocity may be safely used for the boundary condition (BC1) so long as the weighted functional is used. For the boundary condition (BC2), the unweighted functional performs better than the weighted one; however, the latter can still be safely used.

3.4. Mixed boundary conditions. The next series of computations studies the effects of using the two boundary conditions (BC1) and (BC2) simultaneously on different parts of the boundary. Four different configurations, as depicted in Figure 1, of mixed boundary conditions were implemented. The ADN theory is a local theory; i.e., it deals with behavior in the neighborhood of points on the boundary and does not apply to mixed boundary condition cases. The computational experiments using the distributions of boundary conditions depicted in Figure 1 are therefore of interest to see how least-squares methods based on both the unweighted and weighted functionals perform in such settings.

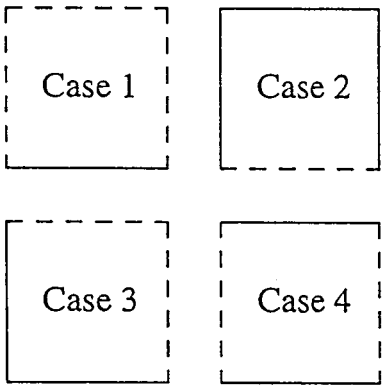

FIG. 1. *Distribution of boundary conditions; solid line for* BC1*, dashed line for* BC2.

TABLE 4
Convergence rates for quadratic-quadratic approximations with mixed boundary conditions.

L^2 error rates								
	Unweighted functional				Weighted functional			
Function	Case 1	Case 2	Case 3	Case 4	Case 1	Case 2	Case 3	Case 4
u	2.88	2.45	2.97	1.95	2.99	3.65	3.07	3.52
v	2.97	2.49	3.15	1.98	3.09	3.40	3.20	3.37
w	2.48	2.11	2.75	1.81	2.90	3.35	3.09	3.50
p	2.58	1.95	2.69	1.81	3.04	3.29	3.11	3.48
H^1 error rates								
	Unweighted functional				Weighted functional			
Function	Case 1	Case 2	Case 3	Case 4	Case 1	Case 2	Case 3	Case 4
u	2.01	1.84	2.02	1.90	2.01	2.16	2.01	2.06
v	2.01	2.10	2.03	1.75	2.01	2.17	2.01	2.14
w	1.91	1.57	1.94	1.64	1.90	2.39	1.93	2.22
p	1.96	1.58	1.98	1.65	1.96	2.40	1.98	2.24

All four mixed boundary condition cases were approximated using both the unweighted functional $\mathcal{J}$ and the weighted functional $\mathcal{J}_h$. In Table 4, we give computed convergence rates in the L^2- and H^1-norms using continuous piecewise quadratic finite element functions for the approximation of all variables. We see that use of the weighted functional yields optimal convergence rates for all four cases. However, use of the unweighted functional results in suboptimal H^1 rates for Cases 2 and 4. It also seems that suboptimal L^2 rates are attained for all four cases, with again Cases 2 and 4 yielding the worst results.

In Table 5, we give computed convergence rates in the L^2- and H^1-norms using continuous piecewise quadratic finite element functions for the velocity approximation and continuous piecewise linear finite element functions for the vorticity and pressure. We see that use of the unweighted functional yields severely suboptimal convergence rates for all four cases. Use of the weighted functional results in much improved approximations, although fully optimal approximations are only obtained for Case 3. In this table, the rates for u seem to differ more widely from those for v than in most of the other tables; we do not have an explanation for this phenomena.

In Table 6, we give computed convergence rates in the L^2- and H^1-norms using

TABLE 5
Convergence rates for quadratic-linear approximations with mixed boundary conditions.

L^2 error rates								
	Unweighted functional				Weighted functional			
Function	Case 1	Case 2	Case 3	Case 4	Case 1	Case 2	Case 3	Case 4
u	1.72	0.42	1.08	0.00	1.88	2.19	3.03	1.29
v	1.79	0.17	1.35	0.29	1.94	2.50	2.87	1.75
w	1.67	0.30	1.07	0.29	1.82	2.06	2.39	1.60
p	1.66	0.31	1.18	0.18	1.95	1.94	2.60	1.34
H^1 error rates								
	Unweighted functional				Weighted functional			
Function	Case 1	Case 2	Case 3	Case 4	Case 1	Case 2	Case 3	Case 4
u	1.58	0.40	0.96	0.14	1.63	2.04	2.30	1.35
v	1.61	0.14	1.29	0.35	1.78	2.15	2.35	1.60
w	0.90	0.20	0.95	0.30	0.91	1.23	1.12	0.93
p	0.96	0.20	0.96	0.43	0.96	1.21	1.15	0.97

continuous piecewise linear finite element functions for the approximation of all variables. For Case 1, one sees that the use of the unweighted functional results in slightly better convergence rates than does use of the weighted functional; however, for Cases 2, 3, and 4, use of the weighted functional results in substantially better convergence rates than does use of the unweighted functional.

The following conclusions can be inferred from our computational experiments. In most cases, use of the weighted functional yields better results, and in all cases it yields "decent" rates of convergence. The unweighted functional can at best be safely used only in Cases 1 and 3; otherwise, serious loss of accuracy occurs. One should note that in Cases 1 and 3 the boundary condition (BC2) is applied on parts of the boundary that are aligned with both coordinate axes while in Cases 2 and 4 that boundary condition is applied only on parts of the boundary that are aligned with a single coordinate axis. One may infer from this the following rule of thumb: the unweighted functional can be safely used (in the sense that any loss of accuracy will not be disastrous) only if the boundary condition (BC2) is applied on parts of the boundary whose normal vectors span $\mathbb{R}^2$. On the other hand, it seems that the weighted functional can be safely used in all cases.

3.5. Mass conservation. Mass conservation, i.e., the satisfaction of the continuity equation, is often a paramount concern of users of computational fluid dynamic algorithms. In [43], it was reported that least-squares finite element methods of the type discussed so far do a very poor job at conserving mass, and a remedy was proposed. Unfortunately, this remedy, which consists of enforcing the continuity equation as an explicit constraint through the use of Lagrange multipliers, defeats one of the main purposes of using least-squares methods! Indeed, one loses the positive definiteness resulting from the least-squares formulation and is led to indefinite problems similar to those that arise in standard mixed-Galerkin methods for the Stokes problem!

Here, we explore, through some computational experiments, the seriousness of the lack of mass conservation in least-squares finite element methods for the Stokes problem. First, we examine the generalized Stokes problem (2.4)–(2.6) with the exact solution (3.1)–(3.3); then we examine the specific problem discussed in [43].

One advantage of least-squares methodologies for systems of equations is that one can, through the introduction of weights, enhance the importance of any equation or

TABLE 6
Convergence rates for linear-linear approximations with mixed boundary conditions.

L^2 error rates								
	Unweighted functional				Weighted functional			
Function	Case 1	Case 2	Case 3	Case 4	Case 1	Case 2	Case 3	Case 4
u	1.65	0.36	0.78	0.50	0.75	1.77	1.36	1.47
v	1.70	0.32	0.97	0.55	0.82	2.00	1.43	1.36
w	1.62	0.30	1.01	0.28	0.85	1.92	1.92	1.49
p	1.59	0.32	1.14	0.19	1.77	1.94	2.30	1.40
H^1 error rates								
	Unweighted functional				Weighted functional			
Function	Case 1	Case 2	Case 3	Case 4	Case 1	Case 2	Case 3	Case 4
u	0.95	0.32	0.75	0.54	0.78	1.16	1.08	0.95
v	0.94	0.13	1.00	0.34	0.81	1.13	1.00	0.94
w	0.90	0.20	0.89	0.30	0.89	1.20	1.03	0.94
p	0.96	0.20	0.91	0.35	0.96	1.20	1.08	0.98

equations (at the expense of the remaining ones, of course.) Thus, if one is interested in enhancing mass conservation, one can use the functional

$$\begin{aligned}\mathcal{J}_{s,K}(\mathbf{u},p,\omega) =& \|\mathbf{curl}\,\omega + \mathbf{grad}\,p - \mathbf{f}_1\|_0^2 \\ &+ Kh^{-s}\|\mathrm{div}\,\mathbf{u} - f_2\|_0^2 + h^{-s}\|\mathrm{curl}\,\mathbf{u} - \omega - f_3\|_0^2\end{aligned} \tag{3.4}$$

with a "large" value for the positive weight K. Note that in terms of the notation we have previously used, $\mathcal{J} = \mathcal{J}_{0,1}$ and $\mathcal{J}_h = \mathcal{J}_{2,1}$.

For the exact solution (3.1)–(3.3), in Table 7, we first give the residual $\|\mathrm{div}\,\mathbf{u}_h - f_2\|_0$ for a 10×10 uniform grid for different values of K and s and for the two types of boundary conditions (BC1) and (BC2), where $\mathbf{u}_h$ denotes the approximate velocity field. As before, in the table, BC1 and BC2 refer to the use of the functional (3.4) without mesh-dependent weights, i.e., with $s = 0$, and BC1w and BC2w refer to the use of the functional (3.4) with mesh-dependent weights, i.e., with $s = 2$. Piecewise quadratic approximations are used for all variables. In Table 7, we also give the rates of convergence for $\|\mathrm{div}\,\mathbf{u}_h - f_2\|_0$.

The column with $K = 1$ corresponds to our previous calculations; i.e., no special treatment of the continuity equation is used. The columns with $K > 1$ correspond to increasing the importance of that equation relative to the remaining ones, while the columns with $K < 1$ correspond to the opposite situation; i.e., the importance of the continuity equation is reduced relative to the other equations.

From the $K = 1$ column, we see, at least for this example, that mass conservation is accomplished to within the expected discretization error. Certainly the rates of convergence are what one expects. If there is any problem, it is with the use of the unweighted functional with the boundary condition (BC1). From the other columns we see that choosing $K > 1$ has little effect except for the case just mentioned; this is probably due to the fact that the residuals are already well within discretization error for the other cases. Choosing $K < 1$, however, can result in a deterioration in the mass conserving ability of the schemes.

We now consider a problem similar to that discussed in [43]. We solve the Stokes system (2.4)–(2.6) with $\mathbf{f}_1 = \mathbf{0}$, $f_2 = 0$, and $f_3 = 0$; note that in this case $\mathrm{div}\,\mathbf{u} = 0$ so that we have the usual continuity equation holding. The computational domain is the rectangle $[-5, 5] \times [-5, 15]$ excluding a circle centered at $(0, 0)$. On the sides of the rectangle, we impose the boundary conditions $u = 1$ and $v = 0$, where u and v

TABLE 7

The residual $\|\text{div}\,\mathbf{u}_h - f_2\|_0$ *for* $h = 0.1$ *and its convergence rate for different values of the weight parameter* K*, for the two boundary conditions* (BC1) *and* (BC2)*, and for the mesh-weighted and unweighted functionals.*

Residual for $h = 0.1$					
K	.01	.1	1	10	100
BC1	1.3914	0.3838	0.0736	0.0255	0.0251
BC1w	0.2004	0.0462	0.0247	0.0237	0.0251
BC2	0.1357	0.0516	0.0286	0.0264	0.0299
BC2w	0.1348	0.0509	0.0285	0.0263	0.0300
Convergence rates					
K	.01	.1	1	10	100
BC1	1.36	1.79	2.02	2.03	2.03
BC1w	2.53	2.76	2.21	2.03	2.13
BC2	1.58	2.14	2.15	2.13	2.15
BC2w	1.59	2.15	2.15	2.13	2.15

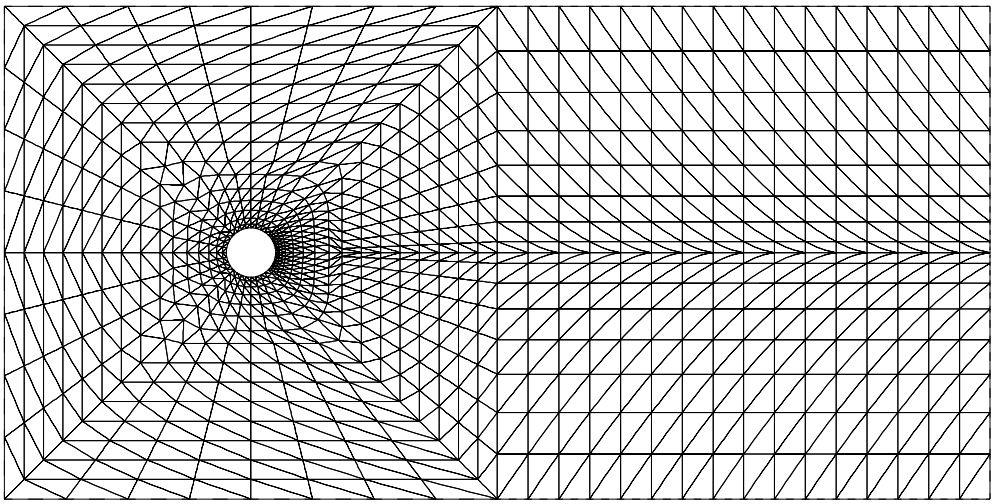

FIG. 2. *Finite element grids for a circle of diameter* 1.

denote the x- and y-components of the velocity; on the circle, we specify $u = v = 0$.

Three different diameters, i.e., 1, 3, and 6, of the circle were used in the numerical study; the grids used in the computations for the three cases are depicted in Figures 2–4, respectively. Note that the same number of grid points is used for all three cases, but, of course, they are redistributed due to the changing size of the circle. Piecewise quadratic approximations are used for all variables.

The amount of mass (assuming a unit density) entering on the left side and exiting from the right side of the rectangle is 10; due to symmetry, we expect that 5 units of mass flows through each of the openings between the circle and the upper and lower sides of the rectangle. Since these openings are of size 4.5, 3.5, and 2 for each of the circles of diameter 1, 3, and 6, respectively, and since the entrance and exit values of the horizontal velocities are 1, we expect that the average value of u along the vertical line segment at the minimum opening, i.e., at $x = 0$ and extending from the circle to the nearest side of the rectangle, to be 10/9, 10/7, and 10/4, respectively.

Five different sets of computational experiments, corresponding to five choices for the least-squares functionals, were conducted. For Case i, we use the unweighted

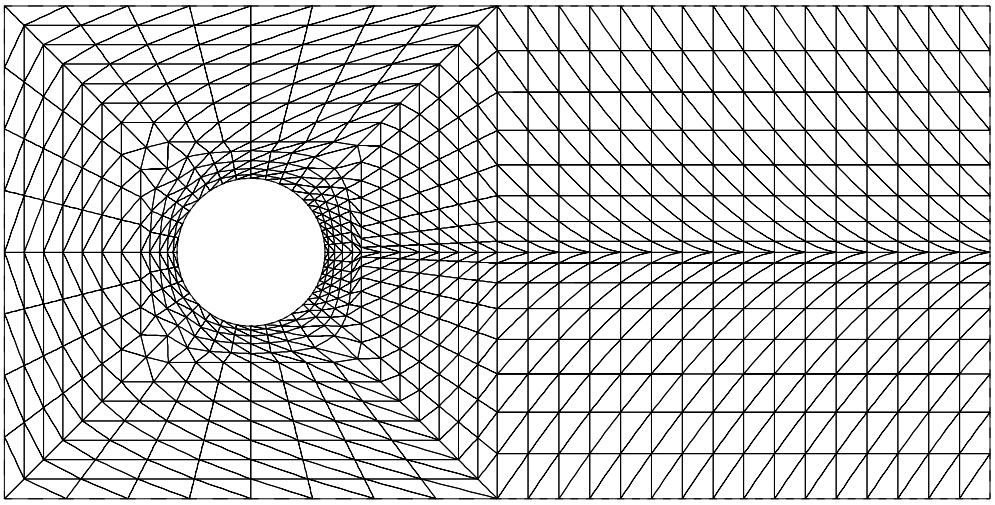

FIG. 3. *Finite element grids for a circle of diameter* 3.

functional $\mathcal{J}_{0,1} = \mathcal{J}$; see (3.4) with $\mathbf{f}_1 = \mathbf{0}$, $f_2 = 0$, and $f_3 = 0$. For Case ii, we use the mesh-weighted functional $\mathcal{J}_{2,1} = \mathcal{J}_h$, where h is chosen as an average grid size; again see (3.4). For Case iii, we use the mesh and continuity equation-weighted functional $\mathcal{J}_{2,10}$, where again h is chosen as an average grid size. The last two cases use the least-squares functional

$$\begin{aligned}\widetilde{\mathcal{J}}_{s,K}(\mathbf{u}, p, \omega) =& \|\mathbf{curl}\,\omega + \mathbf{grad}\,p - \mathbf{f}_1\|_0^2 \\ &+ \sum_j h_j^{-s}\left(K\|\operatorname{div}\mathbf{u} - f_2\|_{0,\Delta_j}^2 + \|\operatorname{curl}\mathbf{u} - \omega - f_3\|_{0,\Delta_j}^2\right),\end{aligned} \tag{3.5}$$

where the sum is taken over the finite elements, Δ_j denotes the jth finite element, h_j denotes the diameter of Δ_j, and $\|\cdot\|_{0,\Delta_j}$ denotes the $L^2(\Delta_j)$-norm. The functional defined in (3.5) allows for mesh-dependent weighting that varies from triangle to triangle, while the functional defined in (3.4) only allows mesh-dependent weighting that is fixed for all triangles. For Case iv, we use the locally mesh-weighted functional $\widetilde{\mathcal{J}}_{2,1}$, while for Case v we use the locally mesh-weighted and continuity equation-weighted functional $\widetilde{\mathcal{J}}_{2,10}$.

Results for the five different choices for the least-squares functional are given in Table 8. The computed masses flowing through each of the openings between the circle and the upper and lower sides of the rectangle are compared, for all five cases and for all three sizes for the circle, with its expected value. Also, the computed average values of u along the vertical line segment at the minimum opening are compared with its expected values.

We see that for the small circle of diameter 1, i.e., for a relatively large opening above and below the circle, that nearly the correct amount of mass and nearly the correct average velocity is achieved. However, as the opening becomes constricted, i.e., as the circle gets larger, mass conservation is less well achieved, especially for the unweighted functional of Case i. Adding mesh-dependent weights improves the situation, although not as much as adding both mesh and continuity equation-dependent weights. There seems to be little difference between using global or local mesh-dependent weights.

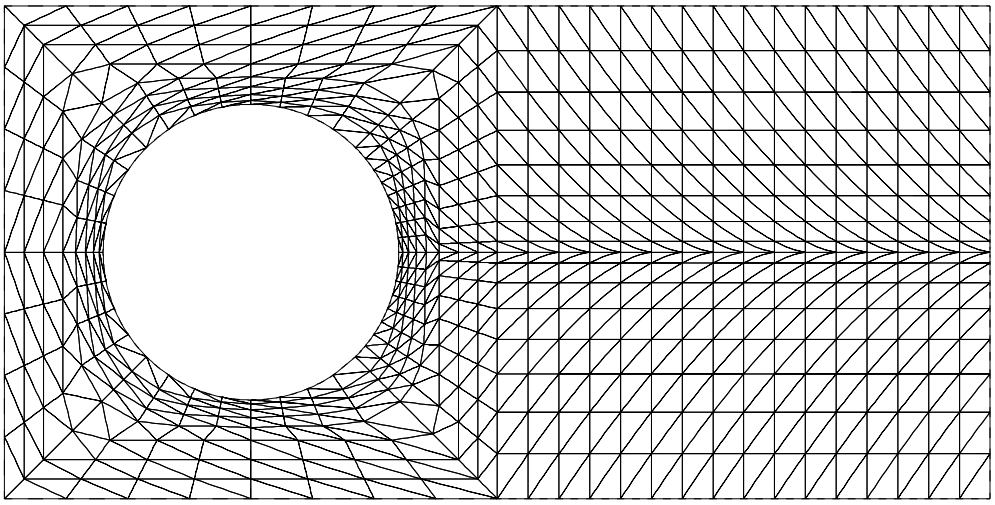

FIG. 4. *Finite element grids for a circle of diameter* 6.

TABLE 8
Mass passing above or below circle and average velocity along vertical line segment above or below circle.

Mass						
Diameter	Expected	Case i	Case ii	Case iii	Case iv	Case v
1	5	4.9469	4.9720	4.9918	4.9671	4.9918
3	5	4.9322	4.9556	4.9868	4.9511	4.9861
6	5	4.2634	4.5070	4.8936	4.4586	4.8868
Average velocity						
Diameter	Expected	Case i	Case ii	Case iii	Case iv	Case v
1	1.1111	1.0993	1.1049	1.1094	1.1038	1.1093
3	1.4285	1.4092	1.4159	1.4247	1.4146	1.4246
6	2.5000	2.1317	2.2535	2.44683	2.2293	2.4434

These observations are reinforced by Figure 5 in which are plotted horizontal velocity profiles along the vertical line segment joining the top of the circle and the upper side of the rectangle. The profiles for all five cases are plotted for the circle of diameter 6, i.e., the configuration giving the poorest results in Table 8. In Figure 5, we see the worst result for the unweighted functional, improved results for locally or globally mesh-dependent weighted functionals, and the best results for the mesh and continuity equation-dependent weighted functionals. Again, we also see that there is little difference in the results for locally or globally mesh-weighted functionals.

To finish our comparisons with the results of [43], in Figure 6 we give the level curves of the horizontal velocity component and, in Figure 7, a vector plot of the velocity field. Both figures are for the worst combination of the unweighted functional, i.e., Case i, and a circle with diameter 6. Even in this worst-case scenario, which is similar to that reported in [43], we do not find the poor mass conservation properties of least-squares finite element methods reported in that article. In fact, Figures 5, 6, and 7 are qualitatively the same as those for the modified method developed in [43] and which leads to nonpositive definite linear systems.

The following conclusions can be drawn from our studies of the mass conservation properties of least-squares finite element methods. First, we do not observe, even for

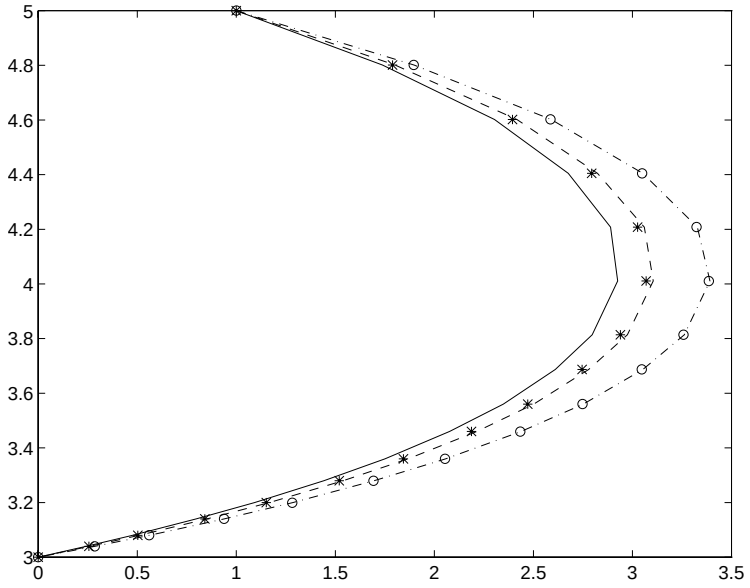

FIG. 5. *Horizontal velocity profile on line segment above the circle.* (*Velocity on horizontal axis, distance along line segment on vertical axis.*) — *Case* i; – – *Case* ii; - · - *Case* iii; * *Case* iv; *and* ∘ *Case* v.

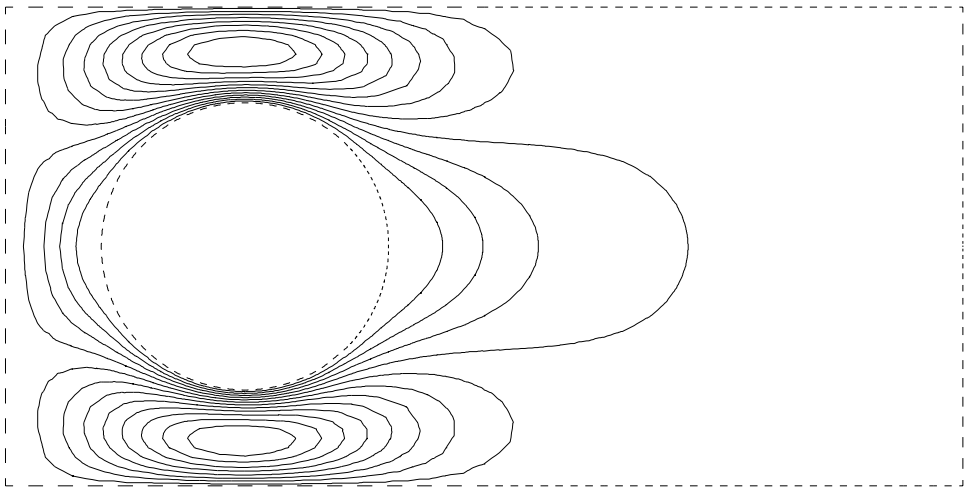

FIG. 6. *Level curves of the horizontal velocity for the unweighted functional and for a circle of radius* 6.

the unweighted functional, the disastrous behavior reported in [43]. Very good results, i.e., of the same quality reported in [43] for the modified, nonpositive definite method developed there, can be easily achieved using weighted functionals without having to give up the favorable property of positive definiteness of the discrete systems.

3.6. Nonconvex polygonal domains. Our next study concerns nonconvex polygonal domains for which solutions are, in general, not smooth. Specifically we will look at an L-shaped domain with one vertex having an interior angle $3\pi/2$. For all variables, we use piecewise quadratic finite element approximations based on both

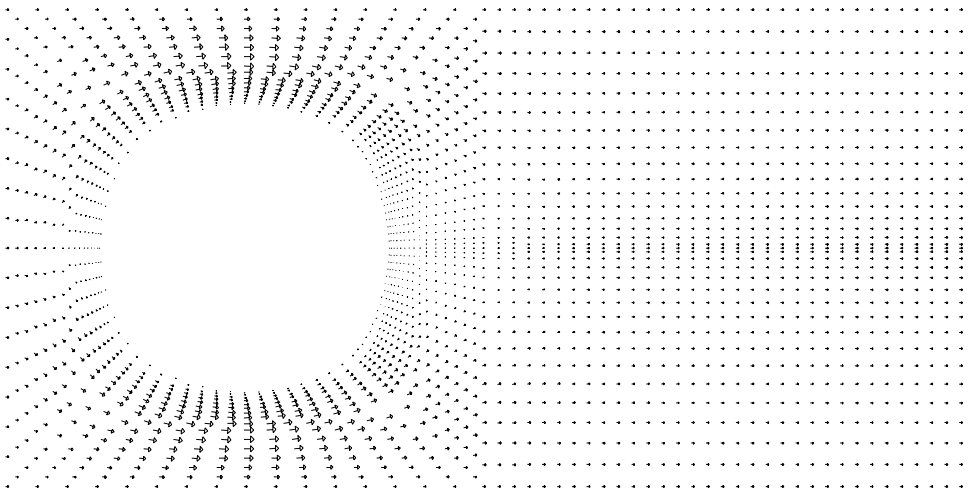

FIG. 7. *The velocity field for the unweighted functional and for a circle of radius* 6.

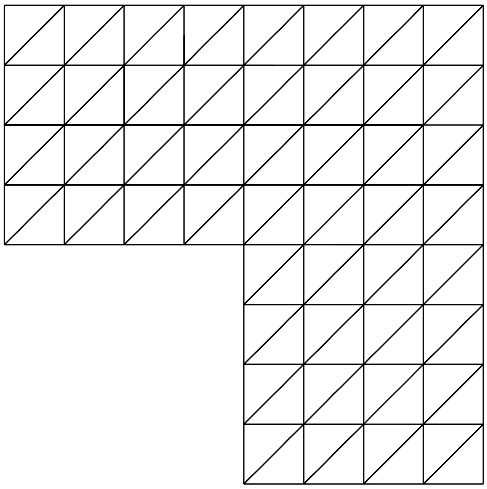

FIG. 8. *Uniform grid for an L-shaped domain.*

uniform meshes and meshes refined in the neighborhood of the re-entrant corner. See Figures 8 and 9 for examples of such grids as well as for the shape of the domain we are considering. For the calculations reported here, the number of grid points used along the longest sides of the L-shaped domain were chosen to be $2, 4, 6, \ldots, 20$.

In order to partially mimic the singularity in the solution that results from applying velocity conditions on the edges meeting at the re-entrant corner, we consider, instead of (3.1)–(3.3), the exact solution

$$\begin{aligned} u = v &= \Phi(x,y) + \sin(\pi x)\sin(\pi y), \\ p &= \Phi(x,y) + \cos(\pi x)\exp^{\pi y}, \\ \omega &= \Phi(x,y) + \sin(\pi x)\exp^{\pi y}, \end{aligned} \tag{3.6}$$

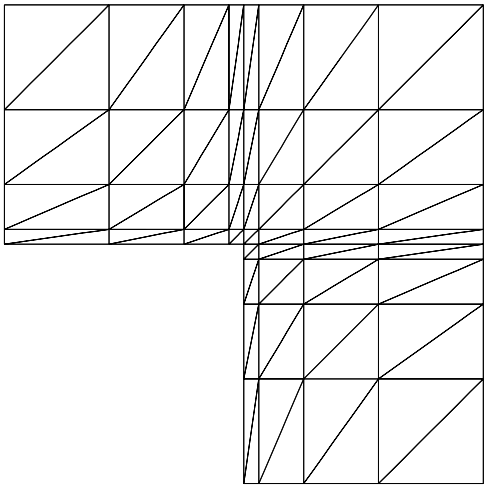

FIG. 9. *Grid refinement near re-entrant corner for an L-shaped domain.*

where

$$\Phi(x,y) = [(x-x_0)^2 + (y-y_0)^2]^{1/3} \sin\left[\frac{1}{3}\tan^{-1}\left(-\frac{x-x_0}{y-y_0}\right)\right].$$

The range of the inverse tangent function is chosen to be $[0, 2\pi]$; also, (x_0, y_0) are the coordinates of the re-entrant corner. The singularity for u and v is what one would expect for the problem at hand; however, the singularities for p and ω are weaker than what one expects from the couplings with u and v appearing in (2.4) and (2.6). We will return to this issue at the end of this section.

The least-squares finite element method employed here is based on the functional $\widetilde{\mathcal{J}}_{s,K}$ (with $K = 1$) defined in (3.5). This allows us, in the nonuniform mesh case, to use mesh-dependent weights which vary from element to element. We also can vary the value of the exponent s in the mesh weighting factor. This flexibility is of interest since it is not clear that the exponent 2 arising from the ADN theory for regular solutions for smooth domains is the best exponent when one deals with the less regular solutions for nonconvex polygonal domains.

In Tables 9 and 10, the results are given for both the boundary conditions (BC1) and (BC2) and for different choices of the exponent s in the functional (3.5). For Table 9, uniform grids of the type depicted in Figure 8 are used, while in Table 10 we use grids that are refined near the re-entrant corner as depicted in Figure 9. In both tables, the L^2 and H^1 convergence rates of the approximate solution is given.

The columns headed by $s = 0$ correspond to the unweighted functional $\widetilde{\mathcal{J}}_{0,1} = \mathcal{J}$. As expected, performance is poor for the boundary condition (BC1) for both the uniform and nonuniform grid cases. For the boundary condition (BC2), it seems, at least for the H^1 error, that grid refinement near the re-entrant corner improves the accuracy of the approximations. The columns headed by $s = 2$ correspond to mesh-dependent weight that would be used for the boundary condition (BC1) on convex domains. For the current configuration of a nonconvex polygonal domain, we see that for that boundary condition we get better accuracy than with the weight exponent $s = 0$; we also see a dramatic improvement if one uses grid refinement near the re-entrant corner. In fact, from Table 10, we see that for the boundary condition

TABLE 9
Convergence rates for a re-entrant corner problem with a uniform grid.

Uniform grid; boundary condition (BC1)								
	L^2 error rates				H^1 error rates			
Function	$s=0$	$s=1$	$s=1.5$	$s=2$	$s=0$	$s=1$	$s=1.5$	$s=2$
u	1.71	2.06	2.04	1.98	1.32	1.37	1.31	1.26
v	2.02	2.04	1.94	1.87	1.40	1.35	1.29	1.25
w	1.87	2.60	2.62	2.44	1.47	2.06	2.16	2.03
p	1.68	2.48	1.09	1.63	1.47	2.06	2.18	2.09
Uniform grid; boundary condition (BC2)								
	L^2 error rates				H^1 error rates			
Function	$s=0$	$s=1$	$s=1.5$	$s=2$	$s=0$	$s=1$	$s=1.5$	$s=2$
u	1.58	1.52	1.33	0.94	1.17	1.17	1.13	0.94
v	1.51	1.45	1.26	0.87	1.14	1.14	1.10	0.91
w	2.21	1.49	0.93	0.42	1.85	1.83	1.72	1.41
p	2.58	2.58	2.58	2.58	1.91	1.91	1.91	1.91

TABLE 10
Convergence rates for re-entrant corner problem with a nonuniform grid.

Refined grid; boundary condition (BC1)								
	L^2 error rates				H^1 error rates			
Function	$s=0$	$s=1$	$s=1.5$	$s=2$	$s=0$	$s=1$	$s=1.5$	$s=2$
u	1.17	2.35	2.81	3.02	0.99	1.71	1.81	1.79
v	1.26	2.28	2.72	2.92	1.15	1.77	1.81	1.79
w	1.26	2.09	2.47	2.78	0.96	1.59	1.83	1.97
p	1.01	2.01	2.39	2.36	0.96	1.59	1.82	1.96
Refined grid; boundary condition (BC2)								
	L^2 error rates				H^1 error rates			
Function	$s=0$	$s=1$	$s=1.5$	$s=2$	$s=0$	$s=1$	$s=1.5$	$s=2$
u	2.65	2.61	2.48	2.11	1.69	1.68	1.68	1.66
v	2.58	2.54	2.39	2.02	1.65	1.65	1.64	1.62
w	2.40	2.36	2.19	1.75	1.56	1.56	1.56	1.54
p	2.44	2.44	2.44	2.44	1.61	1.61	1.61	1.61

(BC1), use of a locally mesh-dependent weight exponent $s = 2$ and grid refinement near the re-entrant corner nearly recovers the optimal accuracy of the approximations. Overall, it seems that for the boundary condition (BC1) the best exponent s seems to be somewhere between 1 and 2, while for the boundary condition (BC2) the best exponent seems to be near 0.

One may be tempted to conclude from these very limited computational experiments that there is some hope of treating singularities arising from nonconvex polygonal domains in the least-squares finite element formalism by using mesh-dependent weights and local grid refinement near re-entrant corners. On the other hand, we have tried to compute with an example for which the ω in (3.6) is replaced with $\operatorname{curl} \mathbf{u}$, where $\mathbf{u}$ is chosen as in (3.6). For this case, we have obtained very poor results, even with grid refinement near the re-entrant corner and different choices for the mesh-dependent weight. More detailed studies are needed in order to ascertain the best mesh weight exponents and grid refinement strategies.

4. Concluding remarks. We conclude with some brief remarks concerning the three dimensional Stokes problem, the nonlinear Navier–Stokes equations, and the condition numbers of the discrete systems. One other remark concerns the use of

quadrature rules. We have found that even for quadratic approximations for all the variables that the three-point midside rule for triangles is sufficiently accurate to preserve the discretization error of least-squares methods based on any of the functionals involving only products of first-order derivatives, e.g., $\mathcal{J}$ and $\mathcal{J}_h$. Indeed, results for the three-point midside rule and a higher-order accurate seven-point rule for triangles are virtually the same.

4.1. The Stokes equations in three dimensions. The velocity-vorticity-(total)-pressure formulation of the (generalized) Stokes equations with velocity boundary conditions in three dimensions is given by

$$\left.\begin{aligned} \mathbf{curl}\,\boldsymbol{\omega} + \mathbf{grad}\,p &= \mathbf{f}_1 \\ \mathbf{curl}\,\mathbf{u} - \boldsymbol{\omega} &= \mathbf{f}_2 \\ \operatorname{div}\mathbf{u} &= f_3 \end{aligned}\right\} \quad \text{in } \Omega \tag{4.1}$$

and

$$\mathbf{u} = \mathbf{U} \qquad \text{on } \Gamma\,. \tag{4.2}$$

Note that the vorticity is now vector valued. Thus, there are seven equations for the seven scalar unknowns consisting of p and the components of $\mathbf{u}$ and $\boldsymbol{\omega}$. This system cannot be elliptic. To remedy this, we add (see [39]) an extra variable ϕ and a seemingly redundant equation to get the elliptic system of eight equations in eight unknowns

$$\left.\begin{aligned} \mathbf{curl}\,\boldsymbol{\omega} + \mathbf{grad}\,p &= \mathbf{f}_1 \\ \operatorname{div}\boldsymbol{\omega} &= -\operatorname{div}\mathbf{f}_2 \\ \mathbf{curl}\,\mathbf{u} + \mathbf{grad}\,\phi - \boldsymbol{\omega} &= \mathbf{f}_2 \\ \operatorname{div}\mathbf{u} &= f_3 \end{aligned}\right\} \quad \text{in } \Omega \tag{4.3}$$

along with the boundary conditions

$$\mathbf{u} = \mathbf{U} \qquad \text{and} \qquad \phi = 0 \qquad \text{on } \Gamma\,. \tag{4.4}$$

It can easily be shown that $\phi = 0$, so that solutions $(\mathbf{u}, \boldsymbol{\omega}, p)$ of (4.3)–(4.4) are indeed solutions of (4.1)–(4.2).

Algorithmically, one can completely ignore ϕ, but one cannot ignore the redundant equation. Thus, one can discretize the problem

$$\left.\begin{aligned} \mathbf{curl}\,\boldsymbol{\omega} + \mathbf{grad}\,p &= \mathbf{f}_1 \\ \operatorname{div}\boldsymbol{\omega} &= -\operatorname{div}\mathbf{f}_2 \\ \mathbf{curl}\,\mathbf{u} - \boldsymbol{\omega} &= \mathbf{f}_2 \\ \operatorname{div}\mathbf{u} &= f_3 \end{aligned}\right\} \quad \text{in } \Omega$$

along with (4.2) using the weighted least squares functional

$$\begin{aligned} \mathcal{J}_h(\mathbf{u}, p, \boldsymbol{\omega}) &= \|\mathbf{curl}\,\boldsymbol{\omega} + \mathbf{grad}\,p - \mathbf{f}_1\|_0^2 + \|\operatorname{div}\boldsymbol{\omega} + \operatorname{div}\mathbf{f}_2\|_0^2 \\ &\quad + h^{-2}\|\mathbf{curl}\,\mathbf{u} - \boldsymbol{\omega} - \mathbf{f}_2\|_0^2 + h^{-2}\|\operatorname{div}\mathbf{u} - f_3\|_0^2 \\ &= \int_\Omega |\mathbf{curl}\,\boldsymbol{\omega} + \mathbf{grad}\,p - \mathbf{f}_1|^2 \, d\Omega + \int_\Omega (\operatorname{div}\boldsymbol{\omega} + \operatorname{div}\mathbf{f}_2)^2 \, d\Omega \\ &\quad + \frac{1}{h^2}\int_\Omega (\mathbf{curl}\,\mathbf{u} - \boldsymbol{\omega} - \mathbf{f}_2)^2 \, d\Omega + \frac{1}{h^2}\int_\Omega (\operatorname{div}\mathbf{u} - f_3)^2 \, d\Omega\,. \end{aligned}$$

The analyses of the Stokes problems in three dimensions based on this functional yields results identical to that obtained in the two-dimensional case.

4.2. The Navier–Stokes equations. The velocity-vorticity-(total)-pressure formulation of the Navier–Stokes equations with velocity boundary conditions in three dimensions is given by

$$\left.\begin{aligned} \nu\mathbf{curl}\,\boldsymbol{\omega} + \boldsymbol{\omega}\times\mathbf{u} + \mathbf{grad}\,p &= \mathbf{f} \\ \mathbf{curl}\,\mathbf{u} - \boldsymbol{\omega} &= \mathbf{0} \\ \operatorname{div}\mathbf{u} &= 0 \end{aligned}\right\} \qquad \text{in } \Omega$$

and

$$\mathbf{u} = \mathbf{U} \qquad \text{on } \Gamma\,,$$

where, if the equations are appropriately nondimensionalized, ν denotes the inverse of the Reynolds number. Computations and preliminary analyses indicate that the best choice of least-squares functional for the Navier–Stokes equations is given by

$$\begin{aligned} \mathcal{J}_h(\mathbf{u},p,\boldsymbol{\omega}) &= \nu^{-2}\|\nu\mathbf{curl}\,\boldsymbol{\omega} + \mathbf{grad}\,p + \boldsymbol{\omega}\times\mathbf{u} - \mathbf{f}\|_0^2 + \nu^{-2}\|\operatorname{div}\boldsymbol{\omega}\|_0^2 \\ &\quad + h^{-2}\|\mathbf{curl}\,\mathbf{u} - \boldsymbol{\omega}\|_0^2 + h^{-2}\|\operatorname{div}\mathbf{u}\|_0^2 \\ &= \frac{1}{\nu^2}\int_\Omega \left|\nu\mathbf{curl}\,\boldsymbol{\omega} + \mathbf{grad}\,p + \boldsymbol{\omega}\times\mathbf{u} - \mathbf{f}\right|^2 d\Omega + \frac{1}{\nu^2}\int_\Omega (\operatorname{div}\boldsymbol{\omega})^2\, d\Omega \\ &\quad + \frac{1}{h^2}\int_\Omega |\mathbf{curl}\,\mathbf{u} - \boldsymbol{\omega}|^2\, d\Omega + \frac{1}{h^2}\int_\Omega (\operatorname{div}\mathbf{u})^2\, d\Omega. \end{aligned} \tag{4.5}$$

Thus, in three dimensions we again add the redundant equation $\operatorname{div}\boldsymbol{\omega} = 0$; this does not apply in two dimensions. Note also that the vorticity transport equations and the redundant equations should be weighted with ν^{-2}.

One must choose a method for linearizing the equation. If one uses Newton's method, then in the neighborhood of a solution, the Hessian matrix is not only symmetric but is also positive definite.

Efficient computational solutions of the Navier–Stokes equations, especially at moderate and high values of the Reynolds number, usually require the use of highly nonuniform grids, e.g., to resolve boundary layers. Thus, one might prefer to use locally mesh-dependent weights in the least-squares functional.

In engineering practice, use of the unweighted (with respect to both the mesh and the Reynolds number) functional

$$\begin{aligned} \mathcal{J}(\mathbf{u},p,\boldsymbol{\omega}) &= \|\nu\mathbf{curl}\,\boldsymbol{\omega} + \mathbf{grad}\,p + \boldsymbol{\omega}\times\mathbf{u} - \mathbf{f}\|_0^2 + \|\operatorname{div}\boldsymbol{\omega}\|_0^2 \\ &\quad + \|\mathbf{curl}\,\mathbf{u} - \boldsymbol{\omega}\|_0^2 + \|\operatorname{div}\mathbf{u}\|_0^2 \end{aligned} \tag{4.6}$$

has resulted in very high quality computational results. A possible explanation for this paradox, i.e., that analyses seem to indicate that one should use the functional (4.5) while computations indicate that good results are obtained using the functional (4.6), is that if one chooses $h = O(\nu)$, then the functionals (4.5) and (4.6) differ only by an unimportant constant scale factor; it is indeed the case that one often chooses h to depend on ν, at least locally, e.g., in boundary layers.

4.3. Condition numbers for the discrete Stokes systems. For the least-squares finite element method based on the unweighted functional $\mathcal{J}$ in the case (BC2), i.e., normal velocity and pressure boundary conditions, it is easy to prove that the condition numbers of the discrete systems of linear algebraic equations are $O(h^{-2})$;

this is similar to Galerkin discretizations of the equivalent second-order problems. Our computations confirm this, although in polygonal domains it seems that one has to be careful with the application of the boundary condition on the normal component of the velocity since otherwise the condition numbers can be severely affected.

A naive estimate for the condition numbers of the discrete systems resulting from the combination of the velocity boundary condition, i.e., (BC1), and the mesh-weighted functionals, i.e., $\mathcal{J}_h$, indicates that the condition number may be as bad as $O(h^{-4})$. Our computational study of this issue is inconclusive, although it seems that the condition number for this case is certainly worse than $O(h^{-2})$. However, further studies indicate that the situation is not so serious. First, introducing a simple diagonal preconditioning, i.e., rescaling all the equations and unknowns by the inverse of the square root of the diagonal elements of the coefficient matrix of the discrete systems results in $O(h^{-2})$ condition numbers. Second, for the Stokes equations in two dimensions, even without diagonal precondition, use of the mesh and Reynolds number-weighted functional (4.5) (with the term $\boldsymbol{\omega} \times \mathbf{u}$ removed) with the choice $h = O(\nu)$ also seemingly results in $O(h^{-2})$ condition numbers. Since this latter scenario is the most likely one for the Navier–Stokes case, the use of mesh-weighted functionals may not lead to serious conditioning problems.

REFERENCES

[1] S. Agmon, A. Douglis, and L. Niremberg, *Estimates near the boundary for solutions of elliptic partial differential equations satisfying general boundary conditions* II, Comm. Pure Appl. Math., 17 (1964), pp. 35–92.

[2] A. Aziz, R. Kellog, and A. Stephens, *Least-squares methods for elliptic systems*, Math. Comp., 10 (1985), pp. 53–70.

[3] A. Aziz and J. Liu, *A weighted least squares method for the backward-forward heat equation,* SIAM J. Numer. Anal., 28 (1991), pp. 156–167.

[4] G. Baker, *Simplified proofs or error estimates for the least-squares method for Dirichlet's problem*, Math. Comp., 27 (1973), pp. 229–235.

[5] B. Bell and K. Surana, *A space time coupled p-version least-squares finite element formulation for unsteady fluid dynamics problems,* Internat. J. Numer. Methods Engrg., 37 (1994), pp. 3545–3569.

[6] P. Bochev, *Analysis of least-squares finite element methods for the Navier-Stokes equations*, SIAM J. Numer. Anal., 34 (1997), pp. 1817–1844.

[7] P. Bochev, Z. Cai, T. Manteuffel, and S. McCormick, *First order least squares for the Navier-Stokes equations,* in Proc. Seventh Copper Mountain Multigrid Conference, NASA Conference Publication 3339, Part 1, 1996, pp. 41–55.

[8] P. Bochev, Z. Cai, T. Manteuffel, and S. McCormick, *Analysis of velocity-flux least-squares principles for the Navier-Stokes equations: Part* I, SIAM J. Numer. Anal., 35 (1998), pp. 990–1009.

[9] P. Bochev and M. Gunzburger, *Least-squares methods for the Navier-Stokes equations*, Appl. Math. Lett., 6 (1993), pp. 27–30.

[10] P. Bochev and M. Gunzburger, *Accuracy of least-squares methods for the Navier-Stokes equations*, Comput. & Fluids, 22 (1993), pp. 549–563.

[11] P. Bochev and M. Gunzburger, *Analysis of least-squares finite element methods for the Stokes equations*, Math. Comp., 63 (1994), pp. 479–506.

[12] P. Bochev and M. Gunzburger, *Analysis of weighted least-squares finite element methods for the Navier-Stokes equations*, in Proc. IMACS 14th World Congress, Georgia Tech, Atlanta, 1994, pp. 584–587.

[13] P. Bochev and M. Gunzburger, *Least-squares methods for the velocity-pressure-stress formulation of the Stokes equations*, Comput. Methods Appl. Mech. Engrg., 126 (1995), pp. 267–287.

[14] J. Bramble, R. Lazarov, and J. Paziak, *A least-squares approach based on a discrete minus one inner product for first order systems*, Math. Comp., to appear.

[15] J. Bramble and J. Paziak, *Least-squares method for Stokes equations based on a discrete minus one inner product,* to appear.

[16] J. Bramble and A. Schatz, *Least-squares methods for* 2*mth order elliptic boundary value problems*, Math. Comp., 25 (1971), pp. 1–32.
[17] Z. Cai, R. Lazarov, T. Manteuffel, and S. McCormick, *First-order system least-squares for partial differential equations: Part* I, SIAM J. Numer. Anal., 31 (1994), pp. 1785–1799.
[18] Z. Cai, T. Manteuffel, and S. McCormick, *First-order system least-squares for velocity-vorticity-pressure form of the Stokes equations, with application to linear elasticity,* ETNA, 3 (1995), pp. 150–159.
[19] Z. Cai, T. Manteuffel, and S. McCormick, *First-order system least-squares for partial differential equations: Part* II, SIAM J. Numer. Anal., 34 (1997), pp. 425–454.
[20] Z. Cai, T. Manteuffel, and S. McCormick, *First-order system least-squares for the Stokes equations, with application to linear elasticity*, SIAM J. Numer. Anal., 34 (1997), pp. 1727–1741.
[21] Z. Cai, T. Manteuffel, S. McCormick, and S. Parter, *First-order system least-squares for planar linear elasticity: Pure traction problem,* SIAM J. Numer. Anal., 35 (1998), pp. 320–335.
[22] Z. Cai and S. McCormick, *Schwarz alternating procedure for elliptic problems discretized by least-squares mixed finite element*, to appear.
[23] Z. Cai and P. Wang, *Least-squares for the velocity-vorticity-pressure formulation for the Stokes problem*, to appear.
[24] Y. Cao and M. Gunzburger, *Least-square finite element approximations to solutions of interface problems*, SIAM J. Numer. Anal., 35 (1998), pp. 393–405.
[25] G. Carey and B. Jiang, *Least-squares finite element method and preconditioned conjugate gradient solution,* Internat. J. Numer. Methods Engrg., 24 (1987), pp. 1283–1296.
[26] G. Carey and B. Jiang, *Least-squares finite elements for first-order hyperbolic systems,* Internat. J. Numer. Methods Engrg., 26 (1988), pp. 81–93.
[27] G. Carey, B. Jiang, and R. Showalter, *A regularization-stabilization technique for nonlinear conservation equations computations,* Num. Methods Partial Differential Equations, 4 (1988), pp. 165–171.
[28] G. Carey, A. Pehlivanov, and Y. Shen, *Least-squares mixed finite elements,* in Finite Element Methods, Proc. Conf. Fifty Years of the Courant Element, M. Kryzek, ed., Jyväskylä, Findland, 1993, pp. 105–107.
[29] G. Carey, A. Pehlivanov, and P. Vassilevski, *Least-squares mixed finite element methods for non-self-adjoint problems:* II. *Performance of block-ILU factorization methods,* SIAM J. Sci. Comput., 16 (1995), pp. 1126–1136.
[30] G. Carey, A. Pehlivanov, and P. Vassilevski, *Least-squares mixed finite element methods for non-self-adjoint problems:* I. *Error estimates,* Numer. Math., 72 (1996), pp. 501–522.
[31] G. Carey and Y. Shen, *Convergence studies of least-squares finite elements for first order systems,* Comm. Appl. Numer. Meth., 5 (1989), pp. 427–434.
[32] C. Chang, *Finite element method for the solution of Maxwell's equations in multiple media,* Appl. Math. Comput., 25 (1988), pp. 89–99.
[33] C. Chang, *A mixed finite element method for the Stokes problem: An acceleration-pressure formulation*, Appl. Math. Comput., 36 (1990), pp. 135–146.
[34] C. Chang, *Finite element approximation for grad-div type systems in the plane*, SIAM J. Numer. Anal., 29 (1992), pp. 425–461.
[35] C. Chang, *An error estimate of the least squares finite element method for the Stokes problem in three dimensions*, Math. Comp., 63 (1994), pp. 41–50.
[36] C. Chang, *An error analysis of least squares finite element method of velocity-pressure-vorticity formulation for Stokes problem: Correction,* Mathematics Research Report 95-53, Department of Mathematics, Cleveland State University, Cleveland, OH, 1995.
[37] C. Chang, *Least squares finite element for second order boundary value problems,* Appl. Math. Comput., to appear.
[38] C. Chang, *A least squares finite element method for incompressible flow in stress-velocity-pressure version,* Comput. Methods Appl. Mech. Engrg., to appear.
[39] C. Chang and M. Gunzburger, *A finite element method for first-order systems in three dimensions*, Appl. Math. Comput., 23 (1987), pp. 171–184.
[40] C. Chang and M. Gunzburger, *A subdomain Galerkin/least squares method for first order elliptic systems in the plane*, SIAM J. Numer. Anal., 27 (1990), pp. 1197–1211.
[41] C. Chang and B. Jiang, *An error analysis of least-squares finite element methods of velocity-vorticity-pressure formulation for the Stokes problem*, Comput. Methods Appl. Mech. Engrg., 84 (1990), pp. 247–255.
[42] C. Chang, J. Li, X. Xiang, Y. Yu, and W. Ni, *Least squares finite element method for electromagnetic fields in* 2*-D,* Appl. Math. Comput., 58 (1993), pp. 143–167.

[43] C. Chang and J. Nelson, *Least-squares finite element method for the Stokes problem with zero residual of mass conservation*, SIAM J. Numer. Anal., 34 (1997), pp. 480–489.
[44] C. Chang, X. Xiang, and J. Li, *An analysis of the eddy current problem by the least squares finite element in* 2*-D,* Appl. Math. Comput., 60 (1994), pp. 179–191.
[45] T. Chen, *On least-squares approximations to compressible flow problems,* Numer. Meth. PDE's, 2 (1986), pp. 207–228.
[46] T. Chen, *Semidiscrete least-squares methods for linear convection-diffusion problems*, Comp. Math. Appl., 24 (1992), pp. 29–44.
[47] T. Chen, *Semidiscrete least-squares methods for linear hyperbolic systems,* Numer. Methods Partial Differential Equations, 8 (1992), pp. 423–442.
[48] T. Chen and G. Fix, *Least Squares Finite Element Simulation of Transonic Flows,* ICASE Report 86-27, NASA Langley Research Center, Hampton, VA, 1986.
[49] P. Ciarlet, *Finite Element Method for Elliptic Problems*, North–Holland, Amsterdam, 1978.
[50] C. Cox and G. Fix, *On the accuracy of least-squares methods in the presence of corner singularities,* Comput. Math. Appl., 10 (1984), pp. 463–476.
[51] C. Cox, G. Fix, and M. Gunzburger, *A least squares finite element scheme for transonic flow around harmonically oscillating airfoils*, J. Comput. Phys., 51 (1983), pp. 387–403.
[52] E. Eason, *A review of least-squares methods for solving partial differential equations,* Internat. J. Numer. Methods Engrg., 10 (1976), pp. 1021–1046
[53] G. Fix and M. Gunzburger, *On least squares approximations to indefinite problems of the mixed type*, Internat. J. Numer. Methods Engrg., 12 (1978), pp. 453–469.
[54] G. Fix, M. Gunzburger, and R. Nicolaides, *On finite element methods of the least-squares type*, Comput. Math. Appl., 5 (1979), pp. 87–98.
[55] G. Fix and E. Stephan, *Finite Element Methods of Least-Squares Type for Regions with Corners,* ICASE Report 81-41, NASA Langley Research Center, Hampton, VA, 1981.
[56] G. Fix and E. Stephan, *On the finite element least squares approximation to higher order elliptic systems,* Arch. Rat. Mech. Anal., 91 (1986), pp. 137–151.
[57] V. Girault and P. Raviart, *Finite Element Methods for Navier-Stokes Equations*, Springer, Berlin, 1986.
[58] R. Glowinski, B. Mantel, J. Periaux, and O. Pironneau, H^{-1} *least squares method for the Navier-Stokes equations,* to appear.
[59] M. Gunzburger, *Finite Element Methods for Viscous Incompressible Flows*, Academic Press, Boston, 1989.
[60] D. Jespersen, *A least-squares decomposition method for solving elliptic equations*, Math. Comput., 31 (1977), pp. 873–880.
[61] B. Jiang *Least-squares finite elements for incompressible Navier-Stokes problems*, Internat. J. Numer. Methods Fluids, 14 (1992), pp. 843–859.
[62] B. Jiang and G. Carey, *Adaptive refinement for least-squares finite elements with element by element conjugate gradient solution,* Internat. J. Numer. Methods Engrg., 24 (1987), pp. 569–580.
[63] B. Jiang and G. Carey, *A stable least-squares finite element method for nonlinear hyperbolic problems,* Internat. J. Numer. Methods Fluids, 8 (1988), pp. 933–942.
[64] B. Jiang and C. Chang, *Least-squares finite elements for the Stokes problem*, Comput. Methods Appl. Mech. Engrg., 78 (1990), pp. 297–311.
[65] B. Jiang, T. Lin, and L. Povinelli, *A Least-Squares Finite Element Method for* 3*D Incompressible Navier-Stokes Equations,* AIAA Report 93-0338, AIAA, New York, 1993.
[66] B. Jiang, T. Lin, and L. Povinelli, *Large-scale computation of incompressible viscous flow by least-squares finite element method*, Comput. Methods Appl. Mech. Engrg., 114 (1995), pp. 213–231.
[67] B. Jiang and L. Povinelli, *Theoretical study of the incompressible Navier-Stokes equations by least-squares methods*, to appear.
[68] B. Jiang and L. Povinelli, *Least-squares finite element method for fluid dynamics*, Comput. Methods Appl. Mech. Engrg., 81 (1990), pp. 13–37.
[69] B. Jiang and V. Sonad, *Least-Squares Solution of Incompressible Navier-Stokes Equations with the p-version of Finite Elements*, NASA TM 105203, ICOMP-91-14, NASA Lewis Research Center, Cleveland, OH, 1991.
[70] B. Jiang, J. Wu, and L. Povinelli, *The Origin of Spurious Solutions in Computational Electromagnetics,* NASA TM-106921 ICOMP-95-8, NASA Lewis Research Center, Cleveland, OH, 1994.
[71] D. Lefebvre, J. Peraire, and K. Morgan, *Least-squares finite element solution of compressible and incompressible flows*, Internat. J. Numer. Methods Heat Fluid Flow, 2 (1992), pp. 99–113.

[72] J. Liable and G. Pinder, *Least-squares collocation solution of differential equations on irregularly shaped domains using orthogonal meshes,* Numer. Methods Partial Differential Equations, 5 (1989), pp. 281–294.
[73] J. Liable and G. Pinder, *Solution of shallow water equations by least squares collocation,* Adv. Water Res., to appear.
[74] P. Lynn and S. Arya, *Use of least-squares criterion in the finite element formulation,* Internat. J. Numer. Methods Engrg., 6 (1973), pp. 75–88.
[75] T. Manteuffel, S. McCormick, and G. Starke, *First-order system least-squares for second-order elliptic problems with discontinuous coefficients,* to appear.
[76] A. Pehlivanov and G. Carey, *Error estimates for least-squares mixed finite elements,* Math. Model Numer. Anal., 28 (1994), pp. 499–516.
[77] A. Pehlivanov and G. Carey, *Convergence studies of least-squares mixed finite element methods,* Comm. Appl. Numer. Methods, to appear.
[78] A. Pehlivanov, G. Carey, and R. Lazarov, *Least-squares mixed finite element methods for second order elliptic problems,* SIAM J. Numer. Anal., 31 (1994), pp. 1368–1377.
[79] A. Pehlivanov, G. Carey, R. Lazarov, and Y. Shen, *Convergence analysis of least-squares mixed finite elements,* Computing, 51 (1993), pp. 111–123.
[80] L. Tang and T. Tsang, *A least-squares finite element method for time-dependent incompressible flows with thermal convection*, Internat. J. Numer. Methods Fluids, to appear.
[81] W. Wedland, *Elliptic Systems in the Plane*, Pitman, London, 1979.
[82] J. Wu, S. Yu, and B. Jiang, *Simulation of Two-Fluid Flows by the Least-Squares Finite Element Method Using a Continuum Surface Tension Model*, Report ICOMP-96-13, NASA Lewis Research Center, Cleveland, OH, 1996.
[83] D. Zeitoun, J. Liable, and G. Pinder, *A weighted least-squares method for first order hyperbolic systems,* to appear.
[84] D. Zeitoun and G. Pinder, *A least squares approach for solving remediation problems of contaminated aquifers,* Numer. Methods Water Resources, to appear.